Integrated In-Silico Approach to Elucidate the Anticholestatic Potential of *Garcinia indica* Choisy Against Clavulanic Acid-Induced cholestasis

Mohammad Zaid Bepari [a], Nayeem A. Khatib [a *], Vishal Patil [a], Shamanand Mallapur [a], Faiz Ahmed Kazi [a]

Email: mozaidb8861@gmail.com

[a]Department of Pharmacology, KLE College of Pharmacy, Belagavi, KLE Academy of Higher Education and Research, Deemed-to-be-University, Belagavi 590010, India.

Corresponding author: Dr. Nayeem A. Khatib

Department of Pharmacology, KLE College of Pharmacy, Belagavi, KLE Academy of Higher Education and Research, Belagavi 590010, India.

Email: nakhatib@klepharm.edu

HIGHLIGHTS

- *Garcinia indica* Choisy phytoconstituents map onto 101 overlapping targets in clavulanic acid-induced cholestasis via network pharmacology
- Isoxanthochymol demonstrates strongest TNF-α binding (-10.0 kcal/mol); apigenin shows highest FXR affinity (-9.1 kcal/mol) among all screened compounds
- MD simulation confirms thermodynamic stability of apigenin-FXR and morelloflavone-HMGCR complexes over 100 ns with persistent catalytic residue contacts
- *G. indica* represents a structurally rational, multi-target natural product candidate for the pharmacological management of drug-induced cholestasis

Abstract

Background and Purpose: Drug-induced cholestasis (DIC), a clinically significant subtype of drug-induced liver injury (DILI), is characterized by impaired bile acid homeostasis, oxidative stress, and progressive hepatocellular damage. Clavulanic acid (CLAV), the primary hepatotoxic component of amoxicillin-clavulanate (AC), disrupts farnesoid X receptor (FXR) and NRF2 signalling while regulatory pathway, leading to impaired BSEP-mediated bile acid transport, activation of inflammatory signalling, and altered cholesterol metabolism through HMGCR dysregulation. Current therapeutic options remain limited in efficacy, creating a need for safer and more effective multi-target approaches. Garcinia indica Choisy, a medicinal plant rich in flavonoids and polyisoprenylated benzophenones, was investigated for its potential anticholestatic activity.

Experimental Approach: 69 phytoconstituents of *G. indica* were screened using ADMET profiling. Network pharmacology analysis was performed to identify overlapping targets associated with clavulanic acid-induced cholestasis. Four key proteins involved in disease progression FXR, BSEP, TNF-α, and HMGCR-were selected for molecular docking studies, followed by 100 ns molecular dynamics simulation to assess complex stability.

Key Results: 24 compounds satisfied the drug-likeness and safety criteria. The identified 101 overlapping targets enriched the pathways related to bile secretion, ABC transporters, cholesterol metabolism, NF-kB signalling, and PI3K-Akt signalling. Docking analysis demonstrated strong binding affinities of apigenin toward FXR (-9.1 kcal/mol), isoxanthochymol toward TNF-α (-10.0 kcal/mol), quercetin toward BSEP (-8.3 kcal/mol), and morelloflavone toward HMGCR (-8.3 kcal/mol). Molecular dynamics simulation further supported the stability of the lead ligand-protein complexes throughout the simulation period.

Conclusion and Implications: The study suggests that *G. indica* phytoconstituents, like apigenin and morelloflavone, may have promising multi-target potential against cholestasis caused by clavulanic acid and further, need to be validated through experimental investigations.

Keywords: clavulanic acid-induced cholestasis; *Garcinia indica*; molecular docking; molecular dynamics; FXR-bile acid homeostasis;

How to cite this article: Bepari MZ, Khatib NA, Patil V, Mallapur S, Kazi FA. Integrated In-Silico Approach to Elucidate the Anticholestatic Potential of Garcinia indica Choisy Against Clavulanic Acid-Induced cholestasis. Int J Drug Deliv Technol. 2026;16(68s):581-594. DOI: 10.25258/ijddt.16.68s.71

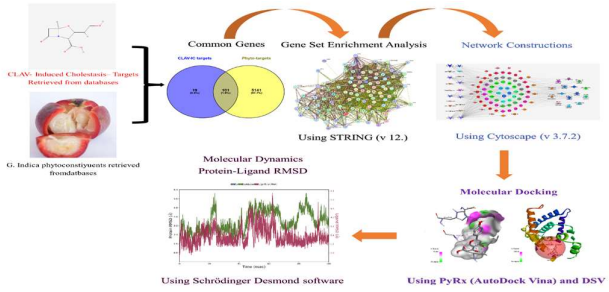

1. Introduction

Drug-induced liver injury (DILI) is one of the main clinical and pharmacological challenge and a leading cause of acute liver failure and post-marketing drug withdrawal worldwide [1, 2]. Drug-induced cholestasis (DIC) is a subtype of DILI, which is characterized by disruption of bile acid (BA) synthesis and transport, leading in intrahepatic accumulation of toxic BA, resulting in oxidative stress, mitochondrial dysfunction, and progressive hepatocellular injury [3, 4]. Antimicrobial, psychiatric medications, anabolic steroids, anti-cancer treatments, and non-steroidal anti-inflammatory drugs (NSAID's) are some of drugs that have been linked to DIC [5].

Antimicrobials are one of the major causes for DILI, where amoxicillin-clavulanate (AC) is implicated as most common cause for DIC, and clavulanic acid (CLAV) is considered to be the primary hepatotoxic component in this combination [6, 7]. AC accounts for 11% of the 24% of antimicrobial-related DILI cases in the DILI network [8, 9]. Mechanistically, CLAV-induced disruption of BA homeostasis is mediated by dysregulation of farnesoid X receptor (FXR) and nuclear factor erythroid 2-related factor 2 (NRF2) signalling [10]. Leading to altered expression of key hepatobiliary transporters and BA synthesis enzymes, which include bile salt export pump (BSEP), sodium taurocholate co-transporting polypeptide (NTCP/SLC10A1), multidrug resistance protein 2 (MDR2/ABCB4), cholesterol 7α-hydroxylase (CYP7A1) and sterol 12α-hydroxylase (CYP8B1) resulting in intrahepatic accumulation of toxic BA and triggering downstream inflammatory and metabolic responses [11]. This accumulation of BA, further amplifies the NF-kB-driven tumor necrosis factor-alpha (TNF-α) signalling leads to inflammatory and metabolic disturbance, leading in altered cholesterol biosynthesis by upregulated 3-hydroxy-3-methylglutaryl-CoA reductase (HMGCR) which exacerbate hepatocellular injury. Collectively, FXR, BSEP, TNF-α, and HMGCR form an integrated regulatory axis linking BA transport, inflammation and metabolic dysregulation, in the progression of DIC [12, 13].

Current therapies for cholestasis focus on enhancing bile flow, reducing BA toxicity, and alleviating symptoms. Ursodeoxycholic acid (UDCA) remains first-line, with obeticholic acid (OCA), an FXR agonist, used in when patient does not respond to UDCA cases, along with symptomatic agents such as cholestyramine and rifampicin. However, due to limited efficacy and adverse effects which includes pruritus, gastrointestinal disturbances, and metabolic complications underscore the need for safer, multi-target therapeutic strategies [14, 15].

In this context, medicinal plants have been emerged as alternative due to their phytochemical diversity and traditional use which may provide a multi-target hepatoprotection. [16, 17]. *Garcinia indica* (*G. indica*) Choisy (kokum; Clusiaceae) has drawn interest as a possible medicinal option. Because of its rich phytochemical profile, which includes flavonoids, phenolics, and anthocyanins, garcinol, hydroxycitric acid, and cyanidin derivatives are some of its important components with antioxidant, anti-inflammatory, hepatoprotective, and metabolic regulating properties [18-20]. Traditionally it has been utilized as a cholagogic and choleretic, suggesting possible importance in cholestatic liver disease [21]. Despite its long-standing traditional use and reported hepatoprotective properties, the molecular mechanisms underlying the therapeutic effects of *Garcinia indica* in DIC remain poorly understood. To bridge this knowledge gap, network pharmacology is employed to elucidate the complex interactions between bioactive phytoconstituents, molecular targets, and disease-associated signaling pathways. Therefore, the present study employed an integrated in silico strategy comprising network pharmacology, molecular docking, molecular dynamics simulations, and LC–MS-based phytochemical validation to investigate the therapeutic potential and mechanistic basis of Garcinia indica against drug-induced cholestasis. [22, 23].

2. Materials and methodology

2.1. *Computational Pharmacology*

2.1.1. Mining of Bioactive Constituents and their Information:

Bioactive compounds of *G. indica* were compiled from published literature and databases, including Dr. Duke's Phytochemical Database (https://phytochem.nal.usda.gov/phytochem/search/list; accessed on 18-09-2025),[24] PCIDB (http://www.genome.jp/db/pcidb; accessed on 18-09-2025), Chemical Entities of Biological Interest (ChEBI) (http://www.ebi.ac.uk/chebi/; accessed on 18-09-2025) [24], and other public repositories. Chemical information was retrieved from the PubChem database (https://pubchem.ncbi.nlm.nih.gov/; accessed on 18-09-2025) [25].

2.1.2. In-silico Druggability Screening and Pharmacokinetic (ADMET) Profiling:

Drug-likeness of the identified phytocompounds was evaluated using Molsoft (http://molsoft.com/mprop/; accessed on 19-09-2025) [25], while ADMET properties were predicted using the pkCSM web server (https://biosig.lab.uq.edu.au/pkcsm/; accessed on 20-09-2025) [26].

2.1.3. In-silico **Druggability Screening and Pharmacokinetic (ADMET) Profiling:**

Potential adverse effects of the retrieved phytoconstituents were predicted based on structural similarity to reference compounds using the ADVERPred web server (http://www.way2drug.com/adverpred/; accessed on 21-09-2025) [25]. Predicted outcomes were expressed as probability of activity (Pa) and probability of inactivity (Pi).

2.1.4. Target Identification for phytocompounds

Target of phytocompounds were retrieved from bindingDB (https://www.bindingdb.org/bind/index.jsp; accessed on 22-09-2025) with a similarity threshold of ≥0.5 [27]. Along with the Comparative Toxicogenomics Database (CTD) (https://ctdbase.org/; accessed on 23-09-2025). SwissTargetPrediction (http://www.swisstargetprediction.ch/; accessed on 23-09-2025) [28].

2.1.5. Target Identification of DIC:

Targets associated with Clavulanic acid were compiled from CTD (https://ctdbase.org/; accessed on 24 September 2025) and Way2Drug (PASS Online; http://www.way2drug.com/passonline/; accessed on 24 September 2025) [24,25]. Whereas, genes related to drug-induced cholestasis were retrieved from GeneCards (https://www.genecards.org/; accessed on 24 September 2025) using the keyword "drug-induced cholestasis", with the search restricted to Homo sapiens and filtered using a relevance score threshold (≥30) to ensure high-confidence associations [27,29]. All gene lists were standardized to official gene symbols, consolidated, and screened to remove duplicate entries. The curated datasets were then comparatively analysed using Venny 2.1 (https://bioinfogp.cnb.csic.es/tools/venny/) to identify genes common to both datasets.

The resulting gene set was considered to represent CLAV-induced cholestasis (CLAV-IC) relevant targets, reflecting molecular components that are both associated with CLAV and implicated in DIC pathology. The final dataset was organized using Microsoft Excel and Venny 2.1 and subsequently used for comparative analysis with the predicted targets of *G.indica* phytoconstituents. These targets were subsequently used for downstream network and pathway analysis.

2.1.6. Gene Set Enrichment Analysis.

Functional enrichment analysis of the shared target genes was performed using the STRING database (version 12.0; https://string-db.org/; accessed on 25 September 2025), restricted to *Homo sapiens* [27]. Pathway enrichment analysis was subsequently conducted using the KEGG database (https://www.kegg.jp/kegg/pathway.html; accessed on 25 September 2025), applying a false discovery rate (FDR) threshold of ≤0.05 after multiple testing correction [30]. Significantly enriched pathways were used to construct downstream interaction networks.

2.1.7. Network Construction.

A compound-target-pathway interaction network was constructed by importing the intersecting *G.indica*-CLAV-IC targets and enriched pathways into Cytoscape software (version 3.7.2) [31]. In this network, nodes represent bioactive compounds, protein targets, and enriched pathways, while edges denote their interactions. Topological parameters, including node degree, were analyzed using the Network Analyzer plugin. The network was visualized using a circular layout for clarity [32].

2.2. Molecular Docking Studies

2.2.1 Ligand preparation

Based on network pharmacology analysis, four key targets-NR1H4 (FXR), ABCB11 (BSEP), HMGCR, and TNF were selected for molecular docking studies. Selected *G.indica* phytochemicals and corresponding standard reference drugs were used as ligands. The three-dimensional structures of the phytocompounds were retrieved in SDF format from PubChem (https://pubchem.ncbi.nlm.nih.gov/; accessed on 16 October 2025) and converted to PDB format using BIOVIA Discovery Studio Visualizer (2019) [29].

2.2.2. *Protein preparation*

Protein structures of FXR (PDB ID: 1OSH), BSEP (PDB ID: 7DV5), HMGCR (PDB ID: 3CDA), and TNF (PDB ID: 2AZ5) were obtained from the RCSB Protein Data Bank (https://www.rcsb.org/; accessed on 16 October 2025) [27]. The proteins were subsequently prepared using BIOVIA Discovery Studio Visualizer (2019) followed by conversion to PDB format.

2.2.3. *Protein-ligand docking*

Molecular Docking analysis of FXR, BSEP, HMGCR and TNF was carried out using PyRx. The resulting receptor structures were archived in PDBQT format for docking analysis after crystallographic water molecules and heteroatoms were eliminated and Gasteiger charges were assigned. The grid box center for BSEP(7DV5) the box dimensions were 82.236 × 157.8155 × 101.3161 Å, and the grid center were set up at X = 92.648, Y = 122.182, and Z = 99.0542, for TNF(2AZ5) grid centre were X = 13.6879, Y = 71.6059, and Z = 27.0007 the box dimensions were 71.6928 × 67.4813 × 71.3257 Å, similarly FXR (1OSH) was set at X =5.5883, Y = 19.7239, and Z = 43.7500 and its dimensions were 37.2629 × 49.6265 × 56.9602 Å. And for HMGCR(3CDA) grid centre were X = 6.3245, Y = 5.7167, and Z = 5.8150 the box dimensions were 78.7689 × 65.7834 × 67.6 Å. Docking was carried out using an exhaustiveness value of 8. The conformations with the lowest binding energies were chosen for further interaction analysis, and binding affinities for each docking posture were reported in kcal/mol [33, 34]. Discovery Studio Visualizer 2019 was used to further evaluate and show protein-ligand interactions, including hydrophobic contacts and hydrogen bonding [27].

2.2.4. *Assessment of active site*

Active-site residues of the target proteins were identified using The PrankWeb server (https://prankweb.cz/ Retrieved on October 16, 2025) [27]. Which predicts probable binding pockets and druggable regions within protein structures to characterize potential ligand-binding sites.

2.2.5. *Molecular dynamics*

Schrodinger Desmond software was used for a 100 ns molecular dynamics (MD) simulation of the protein/ligand complex (systems) was carried out to determine the stability of the complex generated. The systems were solved using the Simple Point Charge model of water under the periodic boundary condition in a cubic box with side lengths of 10 Å × 10 Å × 10 Å. A counterion solution containing Na+ and Cl-was added to neutralize the systems. Water was confined to its geometry and the bond lengths and bond angles of the heavier atoms were preserved using the SHAKE algorithm. Additionally, the Particle Mesh Ewald method was applied to long-range interactions (beyond 9.0 Å) intended for Coulomb forces. A cutoff of 10 Å was used to calculate the Lennard-Jones forces. The Nosé-Hoover chain thermostat and the Martyna-Tobias-Klein barostat with relaxation times of 1.0 ps and 2.0 ps, respectively, were used to produce the 100 ns trajectory at constant temperature and pressure (300 K, 1.01325 bar) after the systems had been minimized and equilibrated in accordance with their respective Desmond default protocols. For short-range interactions, Coulomb forces were calculated over 9.0 Å. RMSD, RMSF, and radius of gyration (rGyr) were computed for each residue at the conclusion of the manufacturing run. Additionally, the protein/ligand interactions were tracked over the course of the 100 ns simulation to evaluate any stability of the intermolecular connections [27].

3. RESULTS

3.1. Integrated Phytochemical Screening: Drug-Likeness, ADMET (HIA), and Toxicity Evaluation:

69 phytoconstituents of G.*indica* were retrieved and were subjected for computational screening procedure. Drug-likeness score was assessed (DLS) using Molsoft, with DLS threshold of > 0.35. Polyprenylated benzophenones showed highest DLS, where guttiferone I and oblongifolin C with DLS of (1.25) each, followed by xanthochymol (1.18) and guttiferone K (1.15). In contrast, flavonoids exhibited moderate DLS, comprising of quercetin (0.52), kaempferol (0.50), apigenin (0.39) and luteolin (0.38). Further, compounds with ≥50% HIA were retrieved, apigenin (93.25%), isogarcinol (94.28%), isoxanthochymol (94.28%), quercetin (77.21%), and kaempferol (74.29%) were notable examples that demonstrated their potential for systemic bioavailability. Additionally, phytocompounds with Pa of <0.65 for cardiotoxicity, hepatotoxicity, and nephrotoxicity were excluded. Following this toxicity filtering, 24 compounds passed the criteria and were selected for further analysis (Supplementary S1).

3.1.1 Retrieving phytocompounds and their intended protein targets

The 24 phytocompounds were identified and their targets were retrived, with quercetin, apigenin, garcinol, isgarcinol showing the strongest protein-regulatory potential. Most of the other constituents predominantly targeted BCL2, TNF, IL6, NR1H4 and ABCB11 (Supplementary Table S 2).

3.1.2 Retrieving of CLAV-modulated protein targets

CLAV-IC is closely associated with disruption in FXR and NRF2 signalling and inflammatory process. To understand the molecular basis of these effects, a total of potential protein targets related to

CLAV-IC were identified. (Supplementary Table S3).

3.2. Gene Set Enrichment Analysis:

STRING based functional enrichment analysis of 101 common *G.indica*-CLAV-IC genes enriched with 179 pathways, among them 15 relevant to CLAV-IC pathways were selected for further investigation (Fig 1) .Key pathways include bile secretion, cholesterol metabolism, ABC transporters, and signalling cascades such as PI3K-Akt, MAPK, and NF-kB, along with processes related to apoptosis and oxidative stress, all of which are related to the pathogenesis of cholestatic liver injury (Supplementary table 4). Key regulators of BA homeostasis-including FXR, BSEP, OATP1B1, MRP2, CYP7A1, and HMGCR, were prominently enriched in bile secretion, ABC transporters and cholesterol metabolism pathways. The enrichment of pro-inflammatory mediators TNF, IL6, MAPK1, NFKB1, mTOR, antioxidant regulators PPARG, PARP1, AKT1, and cell cycle-associated proteins highlight the interaction between inflammatory, metabolic, and survival pathways. All of these finding suggest a multi-target mechanism that underlies anticholestatic

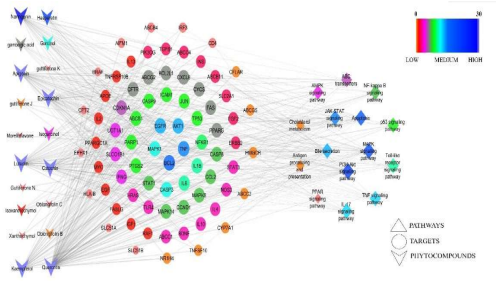

potential of *G. indica* phytoconstituents against CLAV-Induced Cholestasis.

Fig 1. a. Venny representation common genes of CLAV-IC and Phytoconstituents **b.** Protein-protien interaction network showing molecular targets of selected phytoconstituents.

3.3. Compound-Target-Pathway Network Analysis of G. indica Phytoconstituents

Key hub proteins, such as BCL2, TNF, AKT1, TP53, IL6, NFKB1, MAPK1, STAT3, and CASP3, were identified in a compound-target-pathway network built with Cytoscape (Fig 2), emphasizing their functions in inflammation, hepatocellular stress, and cholestatic damage. Polyphenols such as garcinol, gambogic acid, xanthochymol, and guttiferone derivatives, as well as major flavonoids including quercetin, kaempferol, luteolin, apigenin, naringenin, hesperetin, and morelloflavone, demonstrated wide target interactions, indicating multitarget hepatoprotective potential. Pathways linked to bile secretion, cholesterol metabolism, NF-kB, PI3K-Akt, MAPK, JAK-STAT, AMPK, and PPAR signalling were found by enrichment analysis. These

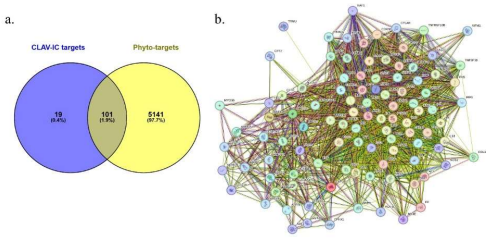

findings suggest that BA imbalance, inflammation, oxidative stress, apoptosis, and immune-mediated liver injury are all coordinated.

Fig 2: Network representation of ***G.indica*** phytocompounds with their probable protein molecules involved in drug-induced cholestasis.

3.4. Molecular docking.

Molecular docking of , TNF, BSEP and HMGCR was carried out with respected interacted phytoconstituent such as quercetin, epicatechin, apigenin, isoxanthochymol. Their binding energies and interaction are summerized in Table 1.

3.4.1. Active site assessment

The PrankWeb server was used to assess the active-site residues of the target proteins. Key residues for BSEP (7DV5) included Gln813, Gln816, Phe820, Thr769, Ala1030, and Ala1036. In TNF (2AZ5), residues such as Tyr151, Leu55, Leu57, Tyr59, and Ile119 were involved across different chains. For FXR (1OSH), the binding pocket comprised His298, Leu291, Ala295, Met332, Ser336, and Trp473. Similarly, active-site residues of HMGCR (3CDA) included Lys692, Asp690, Arg590, Ser684, Met655, and Gly807.

3.4.2. Docking of BSEP(7DV5)

Quercetin (-8.3 kcal/mol) and epicatechin (-8.0 kcal/mol) demonstrated favorable binding for BSEP (ABCB11; PDB ID: 7DV5), a crucial BA efflux transporter. They engaged residues like Gln813, Gln816, Phe820, and Ala103 through hydrogen bonding and hydrophobic interactions involving Asn765, Thr769, and Gly87. Catechin exhibited moderate stabilizing interactions and a relatively lower affinity (-7.3 kcal/mol).

3.4.3. Docking of TNF(2AZ5)

Isoxanthochymol demonstrated the highest binding affinity (-10 kcal/mol) for TNF (PDB ID: 2AZ5), a key mediator of inflammation in cholestatic damage, mostly through hydrophobic interactions with residues like Leu57, Tyr59, and Tyr119. Stable binding was also demonstrated by isogarcinol (-9.3 kcal/mol) and luteolin (-8.9 kcal/mol), which involved hydrophobic interactions and hydrogen bonding with Tyr151 and Arg82.

3.4.4. **Docking of FXR (1OSH)**

Apigenin (-9.1 kcal/mol), quercetin (-9.0 kcal/mol), and kaempferol (-8.9 kcal/mol) were docked with FXR, a crucial regulator of BA homeostasis. These substances demonstrated persistent interactions within the ligand-binding domain, such as hydrogen bonds with residues like

His298, Ser336/337, and hydrophobic contacts with Leu291, Ala295, Met332, and Trp473/474.

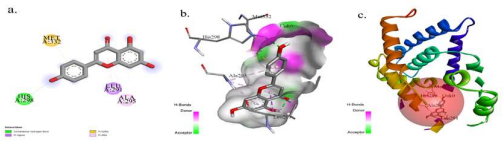

Fig 3: Molecular docking interactions of apigenin with FXR (1OSH). **(a)** 2D ligand interaction diagram illustrating the types and patterns of interactions within the binding site. **(b)** 3D binding pose of apigenin within the catalytic pocket. **(c)** Ribbon representation showing apigenin (pink sphere) docked within the catalytic binding pocket of FXR.

3.4.5. Docking of HMGCR(3CDA)

Quercetin (-8.5 kcal/mol) and morelloflavone (-8.3 kcal/mol) showed persistent binding inside the active site of HMGCR (PDB ID: 3CDA), an important enzyme in cholesterol metabolism and BA precursor production. In addition to hydrophobic contacts including Glu559 and Leu853, interactions included hydrogen bonding with residues like Asp690, Lys692, Asn686, Ser684, Asn658, and Asn810.

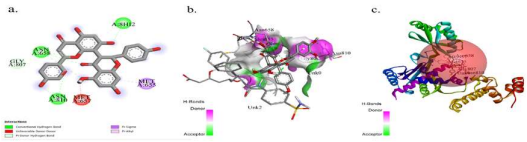

Fig 4: Molecular docking interactions of Morelloflavone with HMGCR (3CDA). **(a)** 2D ligand interaction diagram illustrating the types and patterns of interactions within the binding site. **(b)** 3D binding pose of morelloflavone within the catalytic pocket. **(c)** Ribbon representation showing morelloflavone (pink sphere) docked within the catalytic binding pocket of HMGCR.

Protein Target	Complex	B.E Kcal/Mol	HBI	NHBI	No Of Interactions	Active Site
7DV5	Quercetin	-8.3	Gln813	Trp330,Asn765,Thr769,Ala1030,Ala1036(3)	8	8
	Epicatechin	-8	Gln816,Phe820(2),Ala1034,Thr1038	Gln816,Gly817,Ala821	8	8
	Catechin	-7.3	Gln83,Gln816(2)	Thr326,Ala821,Ser874	6	6
2AZ5	Isoxanthochymol	-10	TyrD:151	Leub:55,Leub:157(2),Leuc:57(3),Tryc:59(2),Ilec:155,Leud:57(3),Tryd:59,Tryd:119	13	12
	Isoganciol	-9.3	TyrB:151	Leua:57(2),Tyra:59,Tyra:119,Tyra:151,Leub:57(2),Tyr:59(2),Tyrb:119	11	11
	Luteolin	-8.9	ArgD:82,LeuD:93	Valb:91,Glnb:125,Vald:91,Leud:93	6	6
1OSH	Apigenin	-9.1	His298	Leu291(2),Ala295(3),Met332	7	7
	Quercetin	-9	Ser337	Leu291(2),Ala295(3),Met332,Trp474	8	8
	Kaempferol	-8.9	Ser336	Leu291(2),Ala295(3),Met332,Trp473	8	8
3CDA	Morelloflavone	-8.3	Asn658(3),Asn810(2),8hi2	Met655,Met657 Gly807,8hi2	10	8
	Quercetin	-8.5	AspA:690,LysA:692,Asn A686,SerA:684,Arg A:590,GlyB:560,	GluB:559,LeuB:853	11	10

			Ser B:565 , Cys B:561, Ala B:751			

Table 1: Binding affinity and molecular interactions of phytocompounds with selected target proteins.

3.5. Molecular Dynamic

3.5.1. Apigenin - 1OSH:

Molecular dynamics simulation of the apigenin-1OSH complex over 100 ns demonstrated stable binding throughout the trajectory. The protein backbone RMSD equilibrated within the first 10 ns and stabilized between 1.6-2.0 Å, with a conformational transition at ~40 ns settling to a lower stable state, indicating induced-fit accommodation of apigenin. Ligand RMSD similarly stabilized after 40 ns (~0.8-1.8 Å), the protein RMSF analysis showed most residues fluctuating below 1.5 Å, with flexibility confined to solvent-exposed loops, while active-site residues remained rigid. Ligand RMSF confirmed apigenin's core flavone scaffold retained structural integrity throughout simulation. Additionally, the radius of gyration (rGyr) profile remained nearly constant throughout the simulation (~3.84-4.0 Å), indicating maintenance of compact protein folding and absence of significant unfolding events. Contact analysis identified Tyr383 (0.59) And Phe298 (0.55) as dominant interacting residues, maintaining persistent hydrophobic and π-stacking contacts, while Asn471 and Ser369 contributed hydrogen bonding. A consistent 4-8 simultaneous contacts were maintained across the entire trajectory, reflecting thermodynamic stability.

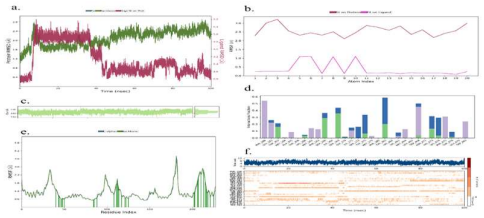

Fig 5: MD trajectories for a 100 ns simulation of Apigenin in combination with FXR (1OSH) (a) RMSD, (b) RMSF, (c) rGyr, and (d, e, f) Ligand-protein contracts based on residues.

3.5.2. HMGCR-Morelloflavone

To assess structural stability and interaction persistence, a 100 ns molecular dynamics simulation of the morelloflavone-HMG-CoA reductase (3CDA) complex was carried out. Throughout the simulation, the protein backbone RMSD showed mild variations between ~2.5-5.5 Å after initially equilibrating within ~10 ns. Interestingly, brief variations between 20-30 ns and 75-90 ns were noted, suggesting conformational rearrangements without total destabilisation. Despite short variations at 50-60 ns, the ligand RMSD was relatively lower (~1.5-3.5 Å) for the most of the journey, indicating steady accommodation inside the binding pocket. With the exception of a small peak close to atom ~46, the fit-on-ligand profile remained below 0.5 Å, indicating modest internal flexibility. Ligand RMSF analysis revealed minimal atomic variations (~0.3-2.2 Å). While active site residues remained stable (<2 Å), protein RMSF showed predicted flexibility in loop areas (~80-100, ~150, ~200, ~250, and ~320 residues), suggesting the preservation of catalytic domain integrity. Key residues, such as Met 658/659, Gln 765, Asp 767, and Glu 806-808, were discovered using interaction analysis. Met 658/659 showed the largest interaction percentage (~2.3), mainly by hydrophobic interactions, while hydrogen bonding was mostly seen with Glu 765, Glu 807, and Thr 808. Ligand stabilisation within the binding pocket was further aided by additional water-bridged interactions. Protein compactness was maintained throughout the simulation, as seen by the rGyr, which stayed constant (~4.45-4.70 Å). Key residues including Met657, Asn658, and Gln766 greatly contributed to interaction stability, and interaction analysis revealed dominating hydrogen bonding and hydrophobic interactions. Sustained ligand binding was supported by persistent contacts that were seen throughout the trajectory, with total interaction counts varying between about 6 and 14.

Fig 6: MD trajectories for a 100 ns simulation of Morelloflavone in combination with HMGCR (3CDA) (a) RMSD, (b) RMSF, (c) rGyr, and (d, e, f)

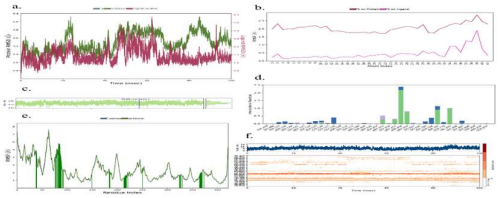

Ligand-protein contracts based on residues.

4. Discussion

The current study demonstrated *Garcinia indica* phytoconstituents may exert anticholestatic effects through coordinated multi-target regulation against clavulanic acid-induced Cholestasis. Among 69 screened compounds, flavonoids such as apigenin, quercetin, kaempferol and polyprenylated benzophenones, including garcinol, isoxanthochymol, isogarcinol showed favorable ADMET profiles and strong binding across key regulators such as BSEP, TNF, FXR and HMGCR. In the case of CLAV-induced Cholestasis, where a single mechanism-FXR inhibition-simultaneously impairs BA synthesis, transport and inflammatory

homeostasis, considering the significance of this multi-target engagement, this phytotherapy may offer a promising and rational therapeutic strategy against cholestasis [10, 11].

The pharmacokinetic profile of *G.indica* phytoconstituents was determined, using a pipeline employed by Mallapur et al(2025) and Patil et al.(2020) where a systematic screening of phytoconstituents was carried out using Molsoft, pkCSM, and ADVERPred, where 24 out of 69 compounds met ADMET requirements [29,32]. These compounds adhered to Lipinski's Rule of Five and demonstrated significant human intestinal absorption (HIA). polyprenylated benzophenones garcinol, isogarcinol, and isoxanthochymol showed high DLS and HIA , probably due to their complex structure and lipophilicity, which is in-consistent with Baliga et al. (2011) and Beerwala et al. (2024, 2025) [18,24,25]. Flavonoids such as apigenin and quercetin also demonstrated appreciable HIA, aligning with Hollmann and katan (1999) and Manach et al (2005) [35, 36]. The therapeutic relevance of these phytoconstituents is further supported by Shou et al. (2020), who noted that favorable ADME characteristics found through in silico screening tend to correlate with improved oral bioavailability and translational potential [37].

101 overlapping targets between CLAV-induced cholestasis genes and *G. indica* phytoconstituents were retrieved and were subjected for KEGG pathway enrichment analysis. The disruption of bile acid transport and hepatic metabolic homeostasis as key events in CLAV-induced cholestasis is highlighted by the enrichment of bile secretion and ABC transporter pathways. The results of Petrov et al. (2021) who showed that clavulanic acid impairs FXR signaling and disrupts bile acid regulatory mechanisms, validate these observations [11]. Furthermore, the involvement of inflammatory pathways is consistent with earlier findings that toxic bile acid accumulation can trigger hepatocyte inflammatory and apoptotic responses. While Faubion et al. (1999) found that toxic bile acid species can directly induce Fas-mediated hepatocyte apoptosis independent of receptor-mediated pathways, Saga et al. (2018) showed that secondary unconjugated bile acids promote hepatic stellate cell activation through inflammatory mediators [13,38]. TNF, AKT1, NFKB1, IL6, and STAT3 were among the hub proteins that were found to be important regulators in the network of compound-target interactions. This further supports the interdependence of inflammatory, metabolic, and transport pathways in CLAV-IC. Significantly, the enrichment of HMGCR, ABCB11, and NR1H4 in these hub clusters supports the selection of these targets during the molecular docking stage. The findings of Xu et al. (2025), who showed that TNF-α-mediated activation of SREBP2 contributes to cholesterol biosynthesis and HMGCR dysregulation under cholestatic conditions, further support this observation by establishing a connection between altered cholesterol metabolism and inflammatory signalling [12]. The network also identified a number of significant phytoconstituents as significant multi-target regulators, such as apigenin, kaempferol, quercetin, luteolin, garcinol, isogarcinol, and isoxanthochymol. Their interaction with proteins involved in inflammatory signaling, cholesterol regulation, and bile transport indicates that G. indica may have anticholestatic effects by simultaneously modulating several interrelated pathways as opposed to a single target mechanism.

BSEP is the principal canalicular transporter involved in bile acid efflux and is considered a key determinant of bile salt-dependent bile flow. According to earlier research by Petrov et al., (2021) clavulanic acid inhibits BSEP expression, which causes intracellular bile acid buildup and subsequent hepatic damage [11]. Quercetin showed the highest binding affinity for BSEP in the current study (-8.3 kcal/mol), interacting through hydrophobic and hydrogen bonding interactions with important active-site residues Gln813, Phe820, Asn765, and Thr769. Additionally, epicatechin and catechin showed favorable binding in the same active pocket. Quercetin's interaction profile closely matches the pharmacophoric model outlined by Jain et al. (2017), indicating a potential transporter-restorative mechanism instead of to an inhibitory one [39]. The overlapping active-site interactions observed for quercetin suggest a potential competitive transporter-restorative mechanism, which is further supported by the in vivo hepatoprotective findings reported by Kabirifar et al., (2017) and the mechanism reported by Wang et al., (2024) where wedelolactone restored BSEP activity through modulation of the FXR-BA-NF-kB/NRF2 axis [40,41]. When BSEP function is disrupted, intracellular bile acid builds up and can cause hepatocellular damage and inflammation by activating the TNF-α and NF-kB signaling pathways [45, 46]. In the current investigation, isoxanthochymol interacted with important trimer interface residues Leu57, Tyr59, and Tyr119 and showed the highest binding affinity toward TNF-α (-10.0 kcal/mol). This binding pattern is in line with the mechanism that He et al. described, in which receptor activation is attenuated by small molecules interfering with TNF trimer assembly. In line with the docking results published by Halder et al. and Agnihotri et al., isogarcinol and luteolin also demonstrated stable interactions at the same interface [44, 45]. Additionally, Chantree et al. (2023) demonstrated that garcinol, a structurally related congener, suppresses NF-kB activation and TNF-α production in macrophages, further supporting the anti-inflammatory potential of G. indica phytoconstituents [46]. Suggesting that isoxanthochymol may attenuate TNF-α and reduce

inflammation. Collectively, these findings suggest a mechanistic cascade in which CLAV-induced BSEP dysfunction drives BA accumulation, subsequently triggering TNF-mediated inflammatory responses that can be restored by *G.indica* phytocompounds.

FXR is a key nuclear receptor that functions through the FXR-SHP-CYP7A1 regulatory pathway to maintain bile acid homeostasis. According to Petrov et al., clavulanic acid exposure inhibits FXR signaling, which causes hepatotoxicity and bile acid buildup [11]. In our study apigenin, quercetin and kaempferol, had showed highest binding affinity to FXR. It interacted with important residues (His298, Ser336/337, Leu291, Ala295, and Met332), the conserved interactions with helix H3 residues Ala295 and His298 are significant as they align with the FXR activation mechanism as reported by Yan et al [47] .Zheng et al. (2021) found that apigenin-mediated FXR activation reduced cholestatic liver injury in vivo, which further supports these findings [48]. Similarly, Xi et al. (2023) showed that by activating the FXR-SHP-CYP7A1 pathway, ligands that target these binding regions increase downstream BSEP and SHP expression [49].

HMGCR, the rate-limiting enzyme of the mevalonate pathway, becomes dysregulated during bile acid-mediated inflammation associated with CLAV-induced disruption of FXR and BSEP signalling [11, 12, 50]. This alteration contributes to increased hepatic cholesterol accumulation and may further aggravate cholestatic injury through enhanced bile acid synthesis. In the present study, quercetin and morelloflavone demonstrated the highest binding affinity toward HMGCR, with docking scores of -8.5 and -8.3 kcal/mol, respectively. Quercetin formed stable interactions with catalytic residues Asp690, Lys692, Asn686, and Ser684, while morelloflavone interacted with Asn658 and Met655/657. These interactions overlap with the substrate-binding region characterised by Istvan and Deisenhofer (2001) and are consistent with the binding profiles reported by Son et al. (2013) [52, 53]. The findings are further supported by Tuansulong et al.,(2011) who identified morelloflavone as an HMGCR inhibitor, and by Riyad et al.,(2023) who demonstrated the cholesterol-lowering effects of quercetin in vivo [54, 55].

The 100 ns molecular dynamics simulation demonstrated that the apigenin-FXR complex remained structurally stable throughout the trajectory. Following an initial equilibration phase within the first 10 ns, the protein backbone RMSD stabilized between 1.6-2.0 Å, while ligand RMSD converged after ~40 ns, indicating stable accommodation of apigenin within the FXR binding cavity. These observations are consistent with the holo-FXR simulations reported by Costantino et al., (2005) where ligand binding reduced conformational fluctuations and stabilized receptor dynamics [55]. A steady radius of gyration (~3.84-4.00 Å) indicates that structural compactness was preserved. Key residues such as Phe298, Tyr383, Leu301, Thr302, Met304, His308, Asn471, and Trp483 drove sustained binding, with His460 exhibiting the highest interaction persistence. Six to eight interactions, mostly hydrophobic, π-π, and water-mediated contacts, were preserved on average. The frequency of histidine-mediated interactions is consistent with both natural FXR agonists like fargesone A.[56] similarly, other QSAR/MD studies emphasizing their function in FXR agonism and stability demonstrated by Yan et al.(2024) and Kumari et al., (2021) [48, 58]. All of these results point to a stable, functionally significant apigenin-FXR complex that may exhibit agonistic behavior. On other hand, in accordance with Son et al, morelloflavone-HMGCR complex displayed more protein backbone variations (RMSD ~2.5-5.5 Å), indicating loop flexibility and an induced-fit binding mechanism [51]. The stability of the rGyr (~4.45-4.70 Å) indicates that the structural integrity was maintained. With predominant hydrophobic interactions at MET residues, key residues (Met657-659, Asn658, Gln765/766, Asp767, Glu806-808) contributed to binding as demonstrated by Azmi et al (2026). The complex was further stabilized by water-mediated interactions and persistent hydrogen bonding (6-14). Interestingly, interactions with catalytic residues Asp767 and Glu806/807 indicate direct enzymatic inhibition, which is in line with previous reports of morelloflavone as a competitive HMGCR inhibitor and crystallographic evidence [55, 56]. Collectively, these findings suggest that morelloflavone may modulate cholesterol production under cholestatic conditions. Together, these simulation results suggest that both flavonoids and polyprenylated benzophenones from *G. indica* maintain stable and conformationally favorable interactions with cholestasis-relevant targets under physiological conditions, providing a mechanistic foundation.

Collectively, these results suggest that several mechanistic pathways involved in clavulanic acid-induced cholestasis may be concurrently modulated by phytoconstituents of Garcinia indica, specifically apigenin, quercetin, isoxanthochymol, and morelloflavone. Restoring FXR-mediated transcriptional regulation, enhancing BSEP-dependent bile acid efflux, suppressing TNF-α-driven inflammatory signaling, and inhibiting HMGCR-associated cholesterol dysregulation are some of their possible actions. According to Hasegawa et al. (2021) and Krupa et al. (2026), such coordinated multi-target activity emphasizes the therapeutic relevance of polypharmacological natural products in complex disorders like CLAV-IC, where currently available therapies like UDCA

and OCA remain limited by variable efficacy and tolerability for their anticholestatic activity [14,15].

However, certain limitations of the present study should be acknowledged. First, the findings are based entirely on computational analyses, and therefore the predicted binding affinities and interaction profiles require further experimental validation through in vitro enzyme inhibition assays, hepatocyte-based bile acid transport studies, and suitable in vivo cholestatic models. Second, although molecular docking using AutoDock Vina provides valuable insights into ligand-protein interactions, it cannot fully account for dynamic protein flexibility, solvent effects, or the entropic contribution to binding under physiological conditions, which may influence the actual binding behaviour of the compounds. In addition, species-specific differences in bile acid metabolism and FXR sensitivity between murine models and humans may affect the translational relevance of the findings. Future studies should therefore focus on validating FXR activation and restoration of BSEP function by the lead phytoconstituents, followed by mechanistic evaluation in experimental models of clavulanic acid-induced cholestasis.

5. Conclusion:

Clavulanic acid-induced cholestasis is a complex form of drug-induced liver injury involving disturbances in bile acid regulation, inflammatory signalling, and cholesterol metabolism. In the present study, an integrated computational approach combining ADMET screening, network pharmacology, molecular docking, and molecular dynamics simulation was employed to evaluate the therapeutic potential of *Garcinia indica* phytoconstituents against these interconnected mechanisms.

Among the screened compounds, apigenin and morelloflavone emerged as the most promising candidates. Apigenin showed stable interaction within the FXR ligand-binding domain, and molecular dynamics analysis further supported its ability to maintain a stable agonistic conformation, suggesting a possible role in restoring the FXR-SHP-CYP7A1 pathway and bile acid homeostasis. Morelloflavone demonstrated favourable binding toward HMGCR and maintained stable interactions with key catalytic residues throughout the simulation, indicating its potential involvement in regulating cholesterol imbalance associated with cholestatic injury.

Overall, the findings suggest that apigenin and morelloflavone may serve as promising multi-target phytoconstituents against clavulanic acid-induced cholestasis. Nevertheless, further experimental validation through in vitro and in vivo studies is required to confirm their therapeutic potential.

Acknowledgements

The authors are grateful to the Head of the Department of Pharmacology and the Principal of KLE College of Pharmacy, KAHER, Belagavi, for providing computational facilities and software needed to complete this research.

Declaration of Competing Interests

The authors report there are no competing interests to declare.

Funding

This research did not receive any specific grant from funding agencies in the public, commercial, or not-for-profit sectors.

Data Availability Statement

The data supporting the findings of this study are available within the article and its supplementary materials. Additional data are available from the corresponding author upon reasonable request.

Ethical Statement

This study did not involve human participants or animal experiments; therefore, no ethical approval was required.

Declaration of Generative AI and AI-Assisted Technologies in the Manuscript Preparation Process

During the preparation of this work the authors used ChatGPT (OpenAI) and Claude (Anthropic) in order to perform grammar correction and language refinement. After using these tools, the authors reviewed and edited the content as needed and take full responsibility for the content of the published article.

Author Contributions

Mohammad Zaid Bepari: Conceptualisation; Data Curation; Methodology; Investigation; Formal Analysis; Writing Original Draft.

Nayeem A Khatib: Conceptualisation; Supervision; Writing-Review and Editing; Project Administration.

Vishal Patil: Methodology; Software; Validation; Writing-Review and Editing.

Shamanand Mallapur: Resources; Writing-Review and Editing; Validation.

Faiz Ahmed Kazi: Data Curation; Writing-Review and Editing.

Supplementary Material:

Table S1: Selected Active Phytocompounds of *Garcinia indica*; Table S2: List of Phytocompounds with their Targets; Table S3: Clavulanic modulated protein targets; Table S4: Drug-likeness and ADMET profiles of 24 selected phytocompounds.

List of Abbreviations

DILI: Drug-induced liver injury; DIC: Drug induced cholestasis; BA: Bile acid: AC Amoxicillin-Clavulanate; CLAV: clavulanic acid; FXR/NR1H4: Farnesoid X receptor; NRF2: Nuclear factor erythroid 2-related factor 2; BSEP/ABCB11: Bile salt export pump; MDR2/ABCB4: Multidrug resistance protein 2; NTCP/SLC10A1: Sodium

taurocholate co-transporting polypeptide; CYP7A1:Cholesterol 7α-hydroxylase; CYP8B1: sterol 12α-hydroxylase; TNF-α/TNF: Tumor necrosis factor-alpha; HMGCR : 3-hydroxy-3-methylglutaryl-CoA reductase; UDCA: Ursodeoxycholic acid; OCA: Obeticholic acid; *G. indica* : *Garcinia indica* CTD: Comparative Toxicogenomics Database; DLS: Drug-likeness score was assessed; HIA: human intestinal absorption; CLAV-IC; CLAV induced cholestasis; BE: Binding energy; HBI: Hydrogen-bond interactions; NHBI: Non-hydrogen-bond interactions; MD: Molecular dynamics; RMSD: Root-mean-square deviation; RMSF: Root-mean-square fluctuation; rGyr: Radius of gyration;; KEGG: Kyoto Encyclopedia of Genes and Genomes; Pa: Probability of activity; Pi: Probability of inactivity; ADMET: Absorption, Distribution, Metabolism, Excretion, and Toxicity; FDR: False discovery rate

6. References

[1] T. Hosack, D. Damry, S. Biswas, Drug-induced liver injury: a comprehensive review, Therap Adv Gastroenterol 16 (2023) 17562848231163410. https://doi.org/10.1177/17562848231163410.

[2] W.M. Lee, Drug-induced Acute Liver Failure, Clin Liver Dis 17 (2013) 10.1016/j.cld.2013.07.001. https://doi.org/10.1016/j.cld.2013.07.001.

[3] N. Kaplowitz, Idiosyncratic drug hepatotoxicity, Nat Rev Drug Discov 4 (2005) 489-499. https://doi.org/10.1038/nrd1750.

[4] N. Chalasani, H. Bonkovsky, R. Fontana, W. Lee, A. Stolz, J. Talwalkar, K. Reddy, P. Watkins, V. Navarro, H. Barnhart, J. Gu, J. Serrano, Features and Outcomes of 899 Patients with Drug-induced Liver Injury: The DILIN Prospective Study, Gastroenterology 148 (2015) 1340-1352.e7. https://doi.org/10.1053/j.gastro.2015.03.006.

[5] J.M. Pinazo-Bandera, J.P. Toro-Ortiz, R.J. Andrade, M. García-Cortés, Drug-induced cholestasis: causative agents and challenges in diagnosis and management, Explor Dig Dis 2 (2023) 202-222. https://doi.org/10.37349/edd.2023.00027.

[6] K.R. Reddy, P. Brillant, E.R. Schiff, Amoxicillin-clavulanate potassium-associated cholestasis, Gastroenterology 96 (1989) 1135-1141. https://doi.org/10.1016/0016-5085(89)91633-8.

[7] Amoxicillin-clavulanic acid therapy may be associated with severe side effects -- review of the literature - PubMed, (n.d.). https://pubmed.ncbi.nlm.nih.gov/11309226/ (accessed April 18, 2026).

[8] AASLD practice guidance on drug, herbal, and dietary supplement-induced liver injury - Fontana - Hepatology - Wiley Online Library, (n.d.). https://onlinelibrary.wiley.com/doi/full/10.1002/hep.32689?msockid=288ed865bbad67fc3f95ced7ba1f6690 (accessed April 17, 2026).

[9] R.J. Andrade, M.I. Lucena, M.C. Fernández, G. Pelaez, K. Pachkoria, E. García-Ruiz, B. García-Muñoz, R. González-Grande, A. Pizarro, J.A. Durán, M. Jiménez, L. Rodrigo, M. Romero-Gomez, J.M. Navarro, R. Planas, J. Costa, A. Borras, A. Soler, J. Salmerón, R. Martin-Vivaldi, Drug-Induced Liver Injury: An Analysis of 461 Incidences Submitted to the Spanish Registry Over a 10-Year Period, Gastroenterology 129 (2005) 512-521. https://doi.org/10.1053/j.gastro.2005.05.006.

[10] S. Modica, R.M. Gadaleta, A. Moschetta, Deciphering the nuclear bile acid receptor FXR paradigm, Nucl Recept Signal 8 (2010) nrs.08005. https://doi.org/10.1621/nrs.08005.

[11] P.D. Petrov, P. Soluyanova, S. Sánchez-Campos, J.V. Castell, R. Jover, Molecular mechanisms of hepatotoxic cholestasis by clavulanic acid: Role of NRF2 and FXR pathways, Food and Chemical Toxicology 158 (2021) 112664. https://doi.org/10.1016/j.fct.2021.112664.

[12] Z. Xu, X. Cao, Z. Zhu, J. Lei, L. Li, X. Zhang, J. Chai, Tumor necrosis factor alpha-induced activation of SREBP2 promotes cholesterol biosynthesis in cholestasis, Biochimica et Biophysica Acta (BBA) - Molecular and Cell Biology of Lipids 1870 (2025) 159642. https://doi.org/10.1016/j.bbalip.2025.159642.

[13] K. Saga, Y. Iwashita, S. Hidano, Y. Aso, K. Isaka, Y. Kido, K. Tada, H. Takayama, T. Masuda, T. Hirashita, Y. Endo, M. Ohta, T. Kobayashi, M. Inomata, Secondary Unconjugated Bile Acids Induce Hepatic Stellate Cell Activation, Int J Mol Sci 19 (2018) 3043. https://doi.org/10.3390/ijms19103043.

[14] S. Hasegawa, M. Yoneda, Y. Kurita, A. Nogami, Y. Honda, K. Hosono, A. Nakajima, Cholestatic Liver Disease: Current Treatment Strategies and New Therapeutic Agents, Drugs 81 (2021) 1181-1192. https://doi.org/10.1007/s40265-021-01545-7.

[15] K.N. Krupa, H. Nguyen, M. Parmar, Obeticholic Acid, in: StatPearls, StatPearls Publishing, Treasure Island (FL), 2026. http://www.ncbi.nlm.nih.gov/books/NBK567735/ (accessed April 22, 2026).

[16] Phytotherapy Research | Medicinal Chemistry Journal | Wiley Online Library, (n.d.). https://onlinelibrary.wiley.com/doi/abs/10.1002/ptr.7821 (accessed April 28, 2026).

[17] Y.H. Gonfa, A. Bachheti, P. Semwal, N. Rai, A.N. Singab, R.K. Bachheti, Hepatoprotective activity of medicinal plants, their phytochemistry, and safety concerns: a systematic review, Z Naturforsch C J Biosci 80 (2025) 61-73. https://doi.org/10.1515/znc-2024-0116.

[18] M.S. Baliga, H.P. Bhat, R.J. Pai, R. Boloor, P.L. Palatty, The chemistry and medicinal uses of the underutilized Indian fruit tree Garcinia indica Choisy (kokum): A review, Food Research International 44 (2011) 1790-1799. https://doi.org/10.1016/j.foodres.2011.01.064.

[19] P. Singh, T.K. Roy, C. Kanupriya, P.C. Tripathi, P. Kumar, K.S. Shivashankara, Evaluation of bioactive constituents of Garcinia indica (kokum) as a potential source of hydroxycitric acid, anthocyanin, and phenolic compounds, LWT 156 (2022) 112999. https://doi.org/10.1016/j.lwt.2021.112999.

[20] Pharmacological Activity of Garcinia indica (Kokum): An Updated Review - PMC, (n.d.). https://pmc.ncbi.nlm.nih.gov/articles/PMC8708457/ (accessed April 22, 2026).

[21] S. Ahmed, M. Zaheer, I.A. Mallick, M.M. Hassan, Choleretic and cholagogic effects of anti-cholelithiatic plants, J Pharmacogn Phytochem 10 (2021) 01-07. https://doi.org/10.22271/phyto.2021.v10.i2a.13664.

[22] S. Harakeh, H.A. Niyazi, H.A. Niyazi, S.A. Abdalal, J.A. Mokhtar, M.S. Almuhayawi, K.K. Alkuwaity, T.S. Abujamel, P. Slama, S. Haque, Integrated Network Pharmacology Approach to Evaluate Bioactive Phytochemicals of *Acalypha indica* and Their Mechanistic Actions to Suppress Target Genes of Tuberculosis, ACS Omega 9 (2024) 2204-2219. https://doi.org/10.1021/acsomega.3c05589.

[23] R. Mazri, M. Ouassaf, A. Zekri, S.U. Khan, K.R.R. Rengasamy, B.Y. Alhatlani, In Silico Network Pharmacology, Molecular Docking, and Molecular Dynamics Analysis of Rosemary-Derived Compounds as Potential HSP90 Inhibitors for Cancer Therapy, CIMB 47 (2025) 860. https://doi.org/10.3390/cimb47100860.

[24] F.A. Beerwala, S.V. Kolambkar, V.S. Patil, H.R. Darasaguppe, N.A. Khatib, V.V. Bhandare, H.V. Hegde, S. Roy, Decoding the alpha-amylase inhibitory activity of Garcinia indica Choisy by computational and experimental studies, South African Journal of Botany 165 (2024) 14-29. https://doi.org/10.1016/j.sajb.2023.12.014.

[25] F.A. Beerwala, S.V. Kolambkar, Adilmehadi. Karikazi, N.A. Khatib, V.V. Bhandare, S. Roy, H.R. Darasaguppe, Harnessing the therapeutic potential of Garcinia indica choisy constituents against olanzapine-induced cardiac and metabolic disorders, In Silico Research in Biomedicine 1 (2025) 100010. https://doi.org/10.1016/j.insi.2025.100010.

[26] H. Yang, C. Lou, L. Sun, J. Li, Y. Cai, Z. Wang, W. Li, G. Liu, Y. Tang, admetSAR 2.0: web-service for prediction and optimization of chemical ADMET properties, Bioinformatics 35 (2019) 1067-1069. https://doi.org/10.1093/bioinformatics/bty707.

[27] V.S. Patil, D.R. Harish, U. Vetrivel, S. Roy, S.H. Deshpande, H.V. Hegde, Hepatitis C Virus NS3/4A Inhibition and Host Immunomodulation by Tannins from Terminalia chebula: A Structural Perspective, Molecules 27 (2022) 1076. https://doi.org/10.3390/molecules27031076.

[28] C. Sucularlı, B. Tozkoparan, S.P. Aytaç, In silico Activity and Target Prediction Analyses of Three Triazolothiadiazine Derivatives, Acta Medica 53 (2022) 251-260. https://doi.org/10.32552/2022.ActaMedica.737.

[29] S.P. Mallapur, B.S. Unger, M.B. Patil, A. Shamnewadi, V.S. Patil, V.P. Japti, Mechanistic insights into the toxicity of Strychnos nuxvomica L. seeds: Shodhana detoxification, 28-day repeated-dose toxicity and computational studies, Toxicol. Environ. Health Sci. 17 (2025) 291-312. https://doi.org/10.1007/s13530-025-00263-x.

[30] A. Shamnewadi, B.S. Unger, P. Palit, S.S. Jalalpure, O. Mali, V.S. Patil, J. Dodakallanavar, H.R. Darasaguppe, S.P. Mallapur, Network pharmacology, molecular docking, molecular dynamics, and ADMET analysis of Curcuma caesia phytoconstituents against rheumatoid arthritis, In Silico Pharmacol. 13 (2025) 161. https://doi.org/10.1007/s40203-025-00454-x.

[31] Q. Zhang, Y. Guo, D. Zhang, Network Pharmacology Integrated with Molecular Docking Elucidates the Mechanism of Wuwei Yuganzi San for the Treatment of Coronary Heart Disease, Natural Product Communications 17 (2022) 1934578X221093907. https://doi.org/10.1177/1934578X221093907.

[32] V.S. Patil, S.H. Deshpande, D.R. Harish, A.S. Patil, R. Virge, S. Nandy, S. Roy, Gene set enrichment analysis, network pharmacology and in silico docking approach to understand the molecular mechanism of traditional medicines for the treatment of diabetes

mellitus, J Proteins Proteom 11 (2020) 297-310. https://doi.org/10.1007/s42485-020-00049-4.

[33] P.F. Ayodele, A. Bamigbade, O.O. Bamigbade, I.A. Adeniyi, E.S. Tachin, A.J. Seweje, S.T. Farohunbi, Illustrated Procedure to Perform Molecular Docking Using PyRx and Biovia Discovery Studio Visualizer: A Case Study of 10kt With Atropine, Prog Drug Discov Biomed Sci 6 (2023). https://doi.org/10.36877/pddbs.a0000424.

[34] V.S. Patil, V.B. Hupparage, H.R. Darasaguppe, S.A. Patil, A.P. Malgi, S. Roy, Indian Journal of Pharmaceutical Sciences, (n.d.). https://www.ijpsonline.com/ (accessed May 4, 2026).

[35] P.C. Hollman, M.B. Katan, Dietary flavonoids: intake, health effects and bioavailability, Food Chem Toxicol 37 (1999) 937-942. https://doi.org/10.1016/s0278-6915(99)00079-4.

[36] C. Manach, G. Williamson, C. Morand, A. Scalbert, C. Rémésy, Bioavailability and bioefficacy of polyphenols in humans. I. Review of 97 bioavailability studies, Am J Clin Nutr 81 (2005) 230S-242S. https://doi.org/10.1093/ajcn/81.1.230S.

[37] W.Z. Shou, Current status and future directions of high-throughput ADME screening in drug discovery, Journal of Pharmaceutical Analysis 10 (2020) 201-208. https://doi.org/10.1016/j.jpha.2020.05.004.

[38] W.A. Faubion, M.E. Guicciardi, H. Miyoshi, S.F. Bronk, P.J. Roberts, P.A. Svingen, S.H. Kaufmann, G.J. Gores, Toxic bile salts induce rodent hepatocyte apoptosis via direct activation of Fas, J. Clin. Invest. 103 (1999) 137-145. https://doi.org/10.1172/JCI4765.

[39] S. Jain, M. Grandits, L. Richter, G.F. Ecker, Structure based classification for bile salt export pump (BSEP) inhibitors using comparative structural modeling of human BSEP, J Comput Aided Mol Des 31 (2017) 507-521. https://doi.org/10.1007/s10822-017-0021-x.

[40] M.-Q. Wang, K.-H. Zhang, F.-L. Liu, R. Zhou, Y. Zeng, A.-L. Chen, Y. Yu, Q. Xia, C.-C. Zhu, C.-Z. Lin, Wedelolactone alleviates cholestatic liver injury by regulating FXR-bile acid-NF-κB/NRF2 axis to reduce bile acid accumulation and its subsequent inflammation and oxidative stress, Phytomedicine 122 (2024) 155124. https://doi.org/10.1016/j.phymed.2023.155124.

[41] R. Kabirifar, Z. Ghoreshi, F. Safari, A. Karimollah, A. Moradi, E. Eskandari-nasab, Quercetin protects liver injury induced by bile duct ligation via attenuation of Rac1 and NADPH oxidase1 expression in rats, Hepatobiliary & Pancreatic Diseases International 16 (2017) 88-95. https://doi.org/10.1016/S1499-3872(16)60164-9.

[42] J.S. Gujral, A. Farhood, M.L. Bajt, H. Jaeschke, Neutrophils Aggravate Acute Liver Injury During Obstructive Cholestasis in Bile Duct-Ligated Mice, Hepatology 38 (2003) 355-363. https://doi.org/10.1053/jhep.2003.50341.

[43] H.-H. Lee, E. Jang, S.-Y. Kang, J.-S. Shin, H.-S. Han, T.-W. Kim, D.H. Lee, J.-H. Lee, D.S. Jang, K.-T. Lee, Anti-inflammatory potential of Patrineolignan B isolated from Patrinia scabra in LPS-stimulated macrophages via inhibition of NF-κB, AP-1, and JAK/STAT pathways, International Immunopharmacology 86 (2020) 106726. https://doi.org/10.1016/j.intimp.2020.106726.

[44] D. Halder, S. Das, A. Joseph, R.S. Jeyaprakash, Molecular docking and dynamics approach to *in silico* drug repurposing for inflammatory bowels disease by targeting TNF alpha, Journal of Biomolecular Structure and Dynamics 41 (2023) 3462-3475. https://doi.org/10.1080/07391102.2022.2050948.

[45] P. Agnihotri, H. Deka, D. Chakraborty, Monu, M. Saquib, U. Kumar, S. Biswas, Anti-inflammatory potential of selective small compounds by targeting TNF-α & NF-kB signaling: a comprehensive molecular docking and simulation study, Journal of Biomolecular Structure and Dynamics 41 (2023) 13815-13828. https://doi.org/10.1080/07391102.2023.2196692.

[46] P. Chantree, P. Martviset, N. Thongsepee, K. Sangpairoj, P. Sornchuer, Anti-Inflammatory Effect of Garcinol Extracted from Garcinia dulcis via Modulating NF-κB Signaling Pathway, Nutrients 15 (2023) 575. https://doi.org/10.3390/nu15030575.

[47] D. Yan, Y. Yang, H. Shen, Z. Liu, K. Yao, Q. Liu, 3D-QSAR and Molecular Dynamics Study of Isoxazole Derivatives to Identify the Structural Requirements for Farnesoid X Receptor (FXR) Agonists, Molecules 29 (2024) 1210. https://doi.org/10.3390/molecules29061210.

[48] S. Zheng, P. Cao, Z. Yin, X. Wang, Y. Chen, M. Yu, B. Xu, C. Liao, Y. Duan, S. Zhang, J. Han, X. Yang, Apigenin protects mice against 3,5-diethoxycarbonyl-1,4-dihydrocollidine-induced cholestasis, Food Funct. 12 (2021) 2323-2334. https://doi.org/10.1039/D0FO02910F.

[49] L. Xi, A. Shi, T. Shen, G. Wang, Y. Wei, J. Guo, Licraside as novel potent FXR agonist for relieving cholestasis: structure-based drug discovery and biological evaluation studies, Front. Pharmacol. 14 (2023) 1197856. https://doi.org/10.3389/fphar.2023.1197856.

[50] Y. Zhang, M. Zhang, S. Fu, Z. Wang, Y. Zhao, J. Gong, M. Chen, N. Zhang, M. Chen, X.Z. Ruan, Y. Chen, Elevated diurnal CD36 expression disrupts the bile acid synthesis rhythm leading to cholestatic liver injury and inflammation via the HMGCR/CYP7A1 axis, Genes & Diseases 13 (2026) 101776. https://doi.org/10.1016/j.gendis.2025.101776.

[51] M. Son, A. Baek, S. Sakkiah, C. Park, S. John, K.W. Lee, Exploration of Virtual Candidates for Human HMG-CoA Reductase Inhibitors Using Pharmacophore Modeling and Molecular Dynamics Simulations, PLoS ONE 8 (2013) e83496. https://doi.org/10.1371/journal.pone.0083496.

[52] E.S. Istvan, J. Deisenhofer, Structural Mechanism for Statin Inhibition of HMG-CoA Reductase, Science 292 (2001) 1160-1164. https://doi.org/10.1126/science.1059344.

[53] K. Tuansulong, N. Hutadilok-Towatana, W. Mahabusarakam, D. Pinkaew, K. Fujise, Morelloflavone from *Garcinia dulcis* as a Novel Biflavonoid Inhibitor of HMG-CoA Reductase, Phytotherapy Research 25 (2011) 424-428. https://doi.org/10.1002/ptr.3286.

[54] P. Riyad, A. Purohit, K. Sen, A. Panwar, H. Ram, HMG - CoA reductase inhibition mediated hypocholesterolemic potential of myricetin and quercetin: *in-silico* and *in-vivo* studies, CyTA - Journal of Food 21 (2023) 115-125. https://doi.org/10.1080/19476337.2022.2162976.

[55] G. Costantino, A. Entrena-Guadix, A. Macchiarulo, A. Gioiello, R. Pellicciari, Molecular dynamics simulation of the ligand binding domain of farnesoid X receptor. Insights into helix-12 stability and coactivator peptide stabilization in response to agonist binding, J Med Chem 48 (2005) 3251-3259. https://doi.org/10.1021/jm049182o.

[56] L. Zhang, Y. Chen, W. Li, Computational Insights into the Interactions of Farnesoid X Receptor with Fargesone A, a Natural Product from Magnolia fargesii, Chem. Res. Chin. Univ. 41 (2025) 146-154. https://doi.org/10.1007/s40242-024-4210-6.

[57] A. Kumari, L. Mittal, M. Srivastava, D.P. Pathak, S. Asthana, Conformational Characterization of the Co-Activator Binding Site Revealed the Mechanism to Achieve the Bioactive State of FXR, Front. Mol. Biosci. 8 (2021) 658312. https://doi.org/10.3389/fmolb.2021.658312.

[58] M. Bilal Azmi, F. Khan, U. Asif, F. Hoda, S. Arslan Sehgal, S. A Qureshi, S.D. Haseen Ahmed, Computational exploration of Withania coagulans-derived natural inhibitors targeting HMG-CoA reductase: A pharmacokinetic, docking and molecular dynamics study for cholesterol regulation in Mus musculus, Pak J Pharm Sci 39 (2026) 999-1020. https://doi.org/10.36721/PJPS.2026.39.4.REG.14438.1.